NASA/CR—1998-208666 UTRC Report 98–07

Deterministic Stress Modeling of Hot Gas Segregation in a Turbine

Judy Busby, Doug Sondak, Brent Staubach, and Roger Davis
United Technologies Research Center,
Pratt & Whitney, East Hartford, Connecticut

October 1998

The NASA STI Program Office . . . in Profile

Since its founding, NASA has been dedicated to the advancement of aeronautics and space science. The NASA Scientific and Technical Information (STI) Program Office plays a key part in helping NASA maintain this important role.

The NASA STI Program Office is operated by Langley Research Center, the Lead Center for NASA's scientific and technical information. The NASA STI Program Office provides access to the NASA STI Database, the largest collection of aeronautical and space science STI in the world. The Program Office is also NASA's institutional mechanism for disseminating the results of its research and development activities. These results are published by NASA in the NASA STI Report Series, which includes the following report types:

- TECHNICAL PUBLICATION. Reports of completed research or a major significant phase of research that present the results of NASA programs and include extensive data or theoretical analysis. Includes compilations of significant scientific and technical data and information deemed to be of continuing reference value. NASA's counterpart of peer-reviewed formal professional papers but has less stringent limitations on manuscript length and extent of graphic presentations.

- TECHNICAL MEMORANDUM. Scientific and technical findings that are preliminary or of specialized interest, e.g., quick release reports, working papers, and bibliographies that contain minimal annotation. Does not contain extensive analysis.

- CONTRACTOR REPORT. Scientific and technical findings by NASA-sponsored contractors and grantees.

- CONFERENCE PUBLICATION. Collected papers from scientific and technical conferences, symposia, seminars, or other meetings sponsored or cosponsored by NASA.

- SPECIAL PUBLICATION. Scientific, technical, or historical information from NASA programs, projects, and missions, often concerned with subjects having substantial public interest.

- TECHNICAL TRANSLATION. English-language translations of foreign scientific and technical material pertinent to NASA's mission.

Specialized services that complement the STI Program Office's diverse offerings include creating custom thesauri, building customized data bases, organizing and publishing research results . . . even providing videos.

For more information about the NASA STI Program Office, see the following:

- Access the NASA STI Program Home Page at ***http://www.sti.nasa.gov***

- E-mail your question via the Internet to help@sti.nasa.gov

- Fax your question to the NASA Access Help Desk at (301) 621-0134

- Telephone the NASA Access Help Desk at (301) 621-0390

- Write to:
  NASA Access Help Desk
  NASA Center for AeroSpace Information
  7121 Standard Drive
  Hanover, MD 21076

NASA/CR—1998-208666 UTRC Report 98–07

Deterministic Stress Modeling of Hot Gas Segregation in a Turbine

Judy Busby, Doug Sondak, Brent Staubach, and Roger Davis
United Technologies Research Center,
Pratt & Whitney, East Hartford, Connecticut

Prepared under Contract NAS3–26618
Task Order 28

National Aeronautics and
Space Administration

Lewis Research Center

October 1998

Acknowledgments

This work was performed with support from NASA Lewis Research Center and funded by the High Performance Computing and Communication Program (HPCCP). The authors appreciate the guidance and support of the NASA Lewis technical monitor, Mr. Joseph Veres. In addition, the authors would like to acknowledge the technical support of Dr. Om Sharma and Dr. Ron-Ho Ni of Pratt & Whitney. Finally, the second author in this effort, Dr. Doug Sondak, is now located at Boston University in the Office of Information Technology.

Available from

NASA Center for Aerospace Information
7121 Standard Drive
Hanover, MD 21076
Price Code: A03

National Technical Information Service
5285 Port Royal Road
Springfield, VA 22100
Price Code: A03

DETERMINISTIC STRESS MODELING OF HOT GAS SEGREGATION IN A TURBINE

Judy Busby, Doug Sondak, Brent Staubach, and Roger Davis
United Technologies Research Center
and Pratt and Whitney
East Hartford, Connecticut 06108

Abstract

Simulation of unsteady viscous turbomachinery flowfields is presently impractical as a design tool due to the long run times required. Designers rely predominantly on steady-state simulations, but these simulations do not account for some of the important unsteady flow physics. Unsteady flow effects can be modeled as source terms in the steady flow equations. These source terms, referred to as Lumped Deterministic Stresses (LDS), can be used to drive steady flow solution procedures to reproduce the time-average of an unsteady flow solution. The goal of this work is to investigate the feasibility of using inviscid lumped deterministic stresses to model *unsteady* combustion hot streak migration effects on the turbine blade tip and outer air seal heat loads using a *steady* computational approach. The LDS model is obtained from an unsteady inviscid calculation. The LDS model is then used with a steady viscous computation to simulate the time-averaged viscous solution.

Both two-dimensional and three-dimensional applications are examined. The inviscid LDS model produces good results for the two-dimensional case and requires less than 10% of the CPU time of the unsteady viscous run. For the three-dimensional case, the LDS model does a good job of reproducing the time-averaged viscous temperature migration and separation as well as heat load on the outer air seal at a CPU cost that is 25% of that of an unsteady viscous computation.

Introduction

Experimental data taken from gas turbine combustors indicates that the flow exiting the combustor has both circumferential and radial temperature gradients. These temperature gradients have significant impact on the wall temperature of the first stage rotor. A combustor hot streak, which can typically have temperatures twice the free stream stagnation temperature, has a greater streamwise velocity and cross-flow vorticity than the surrounding fluid and therefore a larger positive incidence angle to the rotor as compared to the free stream. Due to this rotor incidence variation through the hot streak and the slow convection speed on the pressure side of the rotor, the hot streak typically accumulates on the rotor pressure surface. As a result, the time-averaged rotor-relative stagnation temperature is larger on the pressure surface than on the suction side. The secondary flow in the rotor passage also causes the hot fluid

on the pressure side to spread from midspan towards the hub and tip endwalls, resulting in the heating of the outer air seal.

In the absence of total pressure non-uniformities, the temperature gradients due to the hot streak have minimal impact on the pressure distribution in the rotor. Thus, steady-state computations are typically used to compute the pressure distribution through the first stage of the turbine. For a steady-state computation, the tangential components of the hot streak at the exit of the stator are flux-averaged and only the radial variation in the rotor frame is retained. Many authors have shown that the tangential variations in the hot streak are of prime importance in establishing the hot streak migration path through the blade passage [1,2,3,4]. By mixing out the tangential variation at the rotor inlet, the steady-state computations do not model the temperature segregation in the blade passage or produce the correct temperature distributions on the blade surface.

Previously, the only way to correctly model the hot streak migration through the rotor was with three-dimensional time-accurate viscous computations. However, three-dimensional unsteady viscous computations are too computationally intensive and time consuming to be integrated into the design process. A more desirable approach is to include the time-averaged unsteady effects into a steady computation via an unsteady model. For this work, the lumped deterministic stresses associated with an unsteady inviscid calculation are used to model the time-averaged unsteady effects in a steady viscous calculation. Although unsteady inviscid calculations are more computationally expensive than steady inviscid or viscous computations, they require significantly less computational resources than unsteady viscous computations. Since the migration and segregation of the hot streak in the rotor is predominantly convective in nature, the inviscid LDS field should provide a reasonable model for the time-averaged temperature distribution in the rotor passage. The inviscid LDS models may also provide insight into the development of an analytical model for the unsteady effects.

Both two-dimensional and three-dimensional LDS models are examined in this report. For the two-dimensional application, the LDS model is computed from a 1-1/2 stage turbine *unsteady inviscid* hot streak migration calculation. The corresponding LDS field is first applied to a steady inviscid computation as a check of the overall procedure. Next, the inviscid LDS field is interpolated onto a two-dimensional *viscous* grid and a *steady viscous* solution (with the LDS model) is computed. The inviscid LDS model with the steady viscous solution did a good job of reproducing the viscous time-averaged values of the temperature segregation in the passage and the surface temperature distribution on the blade.

Next, the two-dimensional LDS model is extended to three dimensions. In phase II of this effort, numerous three-dimensional computations for inviscid and viscous steady and unsteady conditions were performed using a strip-blade-strip configuration. For the strip-blade-strip configuration, the first and second vanes were replaced with a narrow (in the axial direction) grid strip. The freestream boundary conditions on these strips were set with the corresponding first vane

exit and second vane inlet conditions. Along with the strip models, various other physical models were used to simulate viscous effects, cooling effects and tip leakage effects. It was determined, however, that these additional physical models produced unrealistic LDS fields and the interaction between the physical and LDS models needs to be investigated further. Therefore, the additional physical models were removed to demonstrate the LDS model by itself and the flow through the stage was recomputed using a vane-blade configuration.

Computational Model

Since deterministic stresses are analogous to turbulent stresses, decomposing velocities into mean and fluctuating components and applying the decomposed velocities to the Navier-Stokes equations is a natural starting point for modeling the deterministic stresses. Consider the 2-D Navier-Stokes equations:

$$\frac{\partial Q}{\partial t}+\frac{\partial E}{\partial x}+\frac{\partial F}{\partial y}-\mathrm{Re}^{-1}\left(\frac{\partial E_v}{\partial x}+\frac{\partial F_v}{\partial y}\right)=0 \tag{1}$$

where Q is the vector of conserved variables, E and F are the convection fluxes, and the diffusion fluxes, E_v and F_v, are given by

$$E_v=\begin{bmatrix}0\\ \tau_{xx}\\ \tau_{xy}\\ e_5^u\end{bmatrix} \qquad F_v=\begin{bmatrix}0\\ \tau_{xy}\\ \tau_{yy}\\ f_5^v\end{bmatrix} \tag{2}$$

where

$$e_5^u=u\tau_{xx}+v\tau_{xy}+q_x \tag{3}$$

$$f_5^v=u\tau_{xy}+v\tau_{yy}+q_y \tag{4}$$

In conventional Reynolds decompositions, velocities are decomposed into mean and fluctuating components, and the stresses τ_{ij} in the above equations represent the sum of molecular stresses and turbulent stresses. In the theory of deterministic stresses [5], the velocity fluctuations are considered to have a random (turbulent) component and a deterministic component. The deterministic fluctuations occur on larger space and time scales than the random fluctuations, and are a result of phenomena such as wake passing and rotor-stator potential interaction. In Ref. [5], the flowfield is further decomposed into an “average passage” and deviations from the average passage, but the average-passage analysis is not employed in the present study.

The velocity is first decomposed into a "deterministic" velocity $\bar{u}$ and a stochastic fluctuation u',

$$u_j = \bar{u}_j + u'_j \tag{5}$$

The deterministic velocity is further decomposed into a mean value and a deterministic fluctuation,

$$\bar{u}_j = \bar{\bar{u}}_j + u''_j \tag{6}$$

This decomposition is illustrated in Fig. 1. The value of is constant, since it is averaged over all time scales. The smooth curve represents temporal variation of the deterministic velocity , which has a relatively large time scale, and the jagged line represents the instantaneous velocity, u.

The decompositions in Eqns. (5) and (6) may be interpreted as using mass-weighted averaging (Favre averaging) or Reynolds averaging. Here, the Navier-Stokes equations are mass-averaged in the conventional manner using Eqn. (5). The velocity is then further decomposed according to Eqn. (6), and the resulting equation is Reynolds averaged. A combination of mass-weighted averaging and Reynolds averaging is employed because this yields a more convenient form of the equations as compared with using either averaging technique alone. These averaging procedures yield two "additional" stress terms,

$$R_{ij} = \overline{\rho u'_i u'_j} + \overline{\bar{\rho} u''_i u''_j} \tag{7}$$

where the first term on the right hand side is the conventional Reynolds stress and the second term on the right hand side is the deterministic stress. The total stress, τ_{ij}, therefore has three components: the molecular stress, the turbulent stress and the deterministic stress.

$$\tau_{ij} = \tau^m_{ij} + \tau^t_{ij} + \tau^d_{ij} \tag{8}$$

Analogous decomposition is also applicable to the heat transfer rate, q_i.

Each diffusion flux in Eqn. (2) can be decomposed into three components in accordance with Eqn. (8). Rewriting Eqn. (1) with this decomposition and explicitly indicating the functional dependence of the fluxes on Q, yields

$$\frac{\partial Q}{\partial t} + \frac{\partial E(Q)}{\partial x} + \frac{\partial F(Q)}{\partial y} - \mathrm{Re}^{-1}\left\{\frac{\partial}{\partial x}\left[E^m_v(Q) + E^t_v(Q) + E^d_v(Q)\right] + \frac{\partial}{\partial y}\left[F^m_v(Q) + F^t_v(Q) + F^d_v(Q)\right]\right\} = 0 \tag{9}$$

Now, define an operator $R(Q)$

$$R(Q) \equiv \frac{\partial E(Q)}{\partial x} + \frac{\partial F(Q)}{\partial y} - \mathrm{Re}^{-1}\left\{\frac{\partial}{\partial x}\left[E_v^m(Q) + E_v^t(Q)\right] + \frac{\partial}{\partial y}\left[F_v^m(Q) + F_v^t(Q)\right]\right\} \qquad (10)$$

Note that this operator does not include the time term or the deterministic stress terms. The sum of the deterministic stress terms in both coordinate directions, D, is defined as

$$D(Q) \equiv -\mathrm{Re}^{-1}\left(\frac{\partial E_v^d(Q)}{\partial x} + \frac{\partial F_v^d(Q)}{\partial y}\right) \qquad (11)$$

Applying Eqns. (10) and (11) to Eqn. (9) yields

$$\frac{\partial Q}{\partial t} + R(Q) + D(Q) = 0 \qquad (12)$$

Let Q_s represent a steady-state solution (without deterministic stresses), and let Q_{ta} represent the time-average of an unsteady solution. Since the numerical approximation of $R(Q)$ is driven toward zero for a steady-state solution,

$$R(Q_s) = 0$$

The time-average of an unsteady solution will not be identical (in general) to the steady-state solution due to the existence of the deterministic stresses. Averaging a periodic flow over one period results in $\partial Q_{ta}/\partial t = 0$ and the deterministic stress term, D, is given by

$$D(Q_{ta}) = -R(Q_{ta})$$

Since the "residual" of the Navier-Stokes solver is the numerical approximation of $R(Q)$, one method of computing $D(Q_{ta})$ is to initialize the flow solver with Q_{ta} and to compute the residual. This, of course, is not a practical method for deducing the deterministic stresses, since the goal is to solve for Q_{ta} without incurring the expense of an unsteady computation, but it is a convenient method for extracting the D field as an aid toward developing a useful model for D. If D could be successfully modeled, it could be input to the solver as a source term and convergence to a steady state would then result in the solution for Q_{ta} without performing an unsteady simulation.

Some unsteady effects are inviscid, such as vane-blade potential interaction, and other unsteady effects are viscous, such as wake shedding. A method for computing the LDS model without performing an unsteady, viscous simulation is

to use an unsteady, *inviscid* simulation instead. The resulting LDS field is interpolated onto the viscous grid, and the viscous simulation is converged to a steady state. This will capture some of the unsteady effects, with the advantage that the cost of the inviscid simulation is significantly less than that for a viscous simulation. Also, the procedure used to compute the LDS model can be used in conjunction with any flow solution procedure.

Flow Solution

The time-dependent, Reynolds-averaged Navier-Stokes equations are solved with an implicit dual time-step approach coupled with a Lax-Wendroff/multiple-grid procedure [4,6,7,8,9]. For the steady computations, only the Lax-Wendroff/multiple-grid procedure is used. The scheme uses central differences for the spatial derivatives with second- and fourth-order smoothing for stability. The algorithm is second-order accurate in time and space. The Baldwin-Lomax [10] turbulence model is used to compute the turbulent viscosity.

No-slip and adiabatic wall conditions are used on all solid boundaries. Giles' [11] two-dimensional, steady, non-reflecting, freestream boundary conditions are used at the downstream freestream boundary. At the inter-blade-row boundaries where the computational grid sectors move relative to each other, the pseudo-time-rate change of the primary variables are interpolated from the adjacent blade row and added to the time-rate changes computed from the Lax-Wendroff treatment.

Results

The results obtained using the two- and three-dimensional inviscid LDS models are presented in this section. For the two-dimensional case, the hot streak migration through 1-1/2 turbine stages is examined. The LDS field resulting from the residual of the time-averaged unsteady inviscid solution is first applied to a steady inviscid solution (to verify that the LDS methodology is implemented correctly). Next, the LDS field is interpolated onto a viscous grid and the subsequent steady viscous solution with the inviscid LDS model is computed.

For the three-dimensional application, the hot streak migration through a single stage is examined. The inviscid LDS field is applied to a steady inviscid solution first and then interpolated onto a viscous grid and applied to a steady viscous solution. The temperature distribution on the blades, outer air seal and through the passage are presented to demonstrate the capabilities of the inviscid LDS model.

Two-Dimensional Analysis

For this analysis, a 1-1/2 stage turbine is modeled with a 1-1-1 blade count. The Euler and viscous grids for the turbine are shown in Fig. 2. Only the flow through the blade sector is examined in detail. To ensure that the LDS source term and methodology are implemented correctly, the inviscid LDS model is added to a steady inviscid computation. By definition of the LDS field (the

residual, or source term, that drives the steady variables to those of the time-averaged solution), the time-averaged solution should be exactly reproduced. The relative temperature on the blade surface for the inviscid steady, time-averaged and LDS solutions is shown in Fig. 3. The LDS model exactly reproduces the time-average temperature distribution on the blade, indicating that the method is implemented correctly.

Next, the LDS field for the inviscid solution is interpolated onto the viscous grid. The energy LDS field through the blade is shown in Fig. 4 for the inviscid grid and interpolated onto the viscous grid. For the hot streak simulations, the LDS field associated with the energy equation dominates the unsteady flow. The effect of the individual components (i.e., continuity, axial and tangential momentum and energy) of the LDS model are shown in Fig. 5. The steady inviscid solution with all of the LDS components is shown on the left. Addition of just the component from the continuity equation produces a very slight temperature segregation, while addition of the momentum terms does not change the temperature distribution from the steady solution. The LDS terms from the energy equation produce nearly all of the temperature segregation in the solution. However, other viscous simulations that did not contain hot streaks [12], showed that the LDS field associated with the other equations may dominate the flow. Thus, all of the LDS terms are used in the inviscid LDS model.

The relative total temperature distribution on the surface of the blade is shown in Fig. 6 for the time-averaged and steady viscous solutions as well as the solution for the steady viscous flow with the inviscid LDS model. The Euler LDS model does a good job of reproducing the viscous time-averaged total temperature distribution on the blade. Figure 7 shows the relative total temperature contours in the passage for the steady and time-averaged viscous solutions and the solution for the steady viscous flow with the inviscid LDS model. This figure shows how well the two-dimensional Euler LDS model reproduces the time-averaged viscous temperature segregation in the passage.

The computational requirements for each case are listed in Table 1. The timings in Table 1 represent 1000 time-steps for the steady case and 10 cycles (where one cycle is the time for one blade to pass one vane) for the unsteady case. The tremendous increase in CPU requirements for the viscous case stems from the need for more time steps per cycle (200 for viscous versus 100 for inviscid) as well as an increase in the number of inner iterations required at each time step to resolve the flow in the viscous region (60 for the viscous versus 25 for the inviscid). The data in Table 1 indicates that the LDS model requires only 3.4% of the CPU time of the unsteady viscous computation.

Table 1. Two-dimensional CPU requirements.

	Total Grid Points	STEADY (CPU sec.)	UNSTEADY (CPU sec.)	TOTAL (CPU sec.)
Inviscid Grid	7,497	598	11,058	11,656
Viscous Grid	72,345	5,773	512,202	517,975
Viscous+Inviscid LDS	72,345	17,429*	N/A	17,429

*CPU=Steady Inviscid+Unsteady Inviscid + Steady Viscous

The results shown in Figs. 6 and 7 indicate that the two-dimensional inviscid LDS model does a good job of reproducing the time-averaged temperature segregation caused by the circumferential variation of the temperature at the inlet to the blade. However, as discussed in a previous section, both the radial and circumferential variations of the temperature affect the migration of the hot streak through the blade sector. As such, it is necessary to examine the three-dimensional application of the LDS model to see if the inviscid LDS model can reproduce the hot streak migration predicted by viscous computations.

Three-Dimensional Analysis

For the three-dimensional computations, an inviscid LDS model is used to simulate the hot streak migration through a single vane-blade stage. The inviscid and viscous grid distributions are shown in Fig. 8. The LDS field is computed from the time-averaged solution obtained with the inviscid grid. The inviscid LDS model is then applied to the corresponding steady inviscid and viscous solutions.

To verify the implementation of the three-dimensional LDS algorithm, the inviscid LDS field from the inviscid grid is added to the corresponding steady inviscid computation. The convergence history for the steady Euler computation with the LDS field is shown in Fig. 9. The convergence history indicates that the steady solver with the inviscid LDS source term is stable and converges in a reasonable time. The relative total temperature distributions on the blade at three spanwise locations for the steady, time-averaged and inviscid LDS model are shown in Fig. 10. The inviscid LDS model exactly reproduces the time-averaged blade surface temperatures at all spanwise locations. Figure 11 shows contours of relative total temperature at midspan in the blade passage. As with the surface temperatures, the inviscid LDS model exactly reproduces the time-averaged temperature segregation in the blade passage. This application of the inviscid LDS model to a steady inviscid problem demonstrates that the LDS methodology is implemented correctly in the three-dimensional solver.

Next, the results from the application of the inviscid LDS model to a steady viscous simulation are presented. The LDS field from an inviscid grid is applied to a steady viscous solution. Since the grid densities differ for the inviscid and viscous grids, the LDS model obtained from the inviscid solution does not map directly onto the viscous grid. Therefore, a three-dimensional interpolation of the inviscid LDS field onto the viscous grid must be performed. The interpolation strategy must be able to handle the difference between inviscid and viscous grid techniques near the leading and trailing edges as well as in the tip clearance

region. The energy LDS fields for the inviscid grid and the viscous grid onto which the LDS field has been interpolated are shown in Fig. 12. The contours at a constant radial plane at midspan are shown on the left, while those for a constant axial plane at the rotor inlet are shown on the right. This figure demonstrates that the three-dimensional interpolator is implemented correctly.

The convergence plot for the steady viscous calculation with inviscid LDS model is shown in Fig. 13, along with the convergence for the steady viscous calculation. The steady solution with the inviscid LDS model requires more iterations to converge, but converges to nearly the same level as the steady viscous computation.

The relative total temperature distributions on the blade for the inviscid LDS model as well as the time-averaged and steady viscous solutions at three spanwise locations are shown in Fig. 14. The inviscid LDS model produces surface temperatures very close to the time-averaged viscous values. Near the endwalls, the inviscid LDS model predicts the same heat loads as the time-averaged viscous solution, but near midspan, the heat load predicted with the inviscid LDS model is less than that of the time-averaged viscous solution. Relative total temperature contours for the rotor pressure and suction surfaces are shown in Fig. 15. The contours indicate that the hot streak predicted with the inviscid LDS model has less spreading of the core region on the pressure surface than that of the time-averaged viscous solution, but matches the time-averaged viscous solution extremely well on the suction side of the blade. Blade-to-blade cuts of the relative total temperature contours at the leading edge of the blade (see Fig. 16) indicate that the inviscid LDS model reproduces the time-averaged viscous temperature segregation near the leading edge that is not produced by the *steady* viscous solution. In Fig. 17, blade-to-blade cuts near midchord show that the core of the hot streak predicted with the LDS model is similar to that predicted with the time-averaged viscous flow, while the steady computation does not produce a core flow at all. However, the core of the hot streak predicted with the LDS model breaks apart near its lower edge with some of the core migrating to the pressure surface and some remaining just off of the pressure surface, resulting in a smaller section of the pressure side of the blade heating up (see Fig. 15, also). The time-averaged viscous solution indicates that the core remains concentrated and all of it migrates to the pressure side of the blade, resulting in a larger area of the pressure side of the blade heating up. Near the trailing edge, (see Fig. 18), the behavior of the core hot streak is similar to that at midchord: The core produced with the LDS model is less concentrated than that of the time-averaged viscous computation, resulting in a smaller area of the blade surface heating up.

The ultimate goal of this work is to predict the effect of the hot streak on the time-averaged temperature distribution on the outer air seal with a steady computation. The circumferentially averaged relative total temperatures on the outer air seal for the steady and time-averaged viscous solutions as well as the steady viscous with the inviscid LDS model are shown in Fig. 19. The steady viscous computation predicts cooler temperatures in the leading edge region than the time-averaged viscous computation. The inviscid LDS model does a

good job of predicting the time-averaged viscous temperature level as well as the location where the outer air seal begins to heat up.

As with the two-dimensional results, the steady viscous solution with the LDS model is significantly less expensive to compute than the unsteady viscous solution. The computational costs for the inviscid, viscous and LDS solutions are shown in Table 2. The CPU times for the steady computations are based on 6000 iterations, while those for the unsteady computations are based on 10 cycles. For the unsteady inviscid and viscous solutions, 200 iterations per global cycle and 10 (for inviscid) and 30 (viscous) inner iterations are used. The CPU requirements for the steady viscous computations with inviscid LDS model are only 25% of those for the unsteady viscous computations. This number is higher than that for the two-dimensional case (3.6%), because a finer inviscid grid is required to resolve the three-dimensional effects.

The results presented in this section indicate that the inviscid LDS model is a viable option for predicting the time-averaged flow characteristics of a hot streak migrating through a turbine stage and the temperature increase on the outer air seal caused by the hot streak. The inviscid LDS model does not exactly reproduce the segregation and spreading of the hot streak core that is predicted by the time-averaged viscous flow. This deficiency may be due to the lack of viscous effects in the inviscid LDS model. Further work is required to incorporate viscous effects into the inviscid LDS model and to examine in detail the LDS field associated with the viscous regions. This could be achieved by comparing the LDS field from a viscous solution with that from an inviscid solution. Performing a parametric study of the application of the LDS models for various hot streak profiles may also indicate the driving mechanism behind the differences in the LDS solution and the time-averaged solution.

The success of the LDS model comes at the relatively low cost of the inviscid solutions. Another approach that may be even less costly is to develop a new inter-blade-row boundary condition that includes the unsteady effects as a source term, similar to the implementation of the LDS model. An analytical description of the source term may also be derived from the lumped deterministic stress terms.

Table 2. Three-dimensional CPU requirements.

	Total Grid Points	STEADY (CPU sec.)	UNSTEADY (CPU sec.)	TOTAL (CPU sec.)
Inviscid Grid	143,418	68,668	169,546	238,514
Viscous Grid	430,122	205,942	1,525,449	1,731,391
Viscous+Inviscid LDS	430,122	444,456*	N/A	444,456

*CPU=Steady Inviscid+Unsteady Inviscid + Steady Viscous

Conclusions

This report has presented the results of a study into the feasibility of using lumped deterministic stresses to model the time-averaged unsteady effects of the migration of a hot streak through a first stage rotor and the resulting heat load on the outer air seal. Time-averaged unsteady inviscid solutions are used to compute the LDS model. This model is then used with a steady viscous solution to simulate the time-averaged viscous solution. Both two-dimensional and three-dimensional models are examined. The two-dimensional results indicate that the inviscid LDS model can simulate the time-averaged viscous solutions at a significant reduction in CPU costs. The three-dimensional results show that the inviscid LDS model does a good job of predicting the migration and segregation of the hot streak as well as the increased heat load on the outer air seal. These three-dimensional results can also be obtained at a significant savings in CPU.

The effect of the tip leakage flow was not included in these computations and should be addressed. Other areas that need to be examined include incorporating viscous effects into the LDS model and developing a new inter-blade-row boundary condition that includes the LDS model for the unsteady effects. Performing a parametric study of the application of the LDS models for various hot streaks would also provide insight into the development of an analytical model. This work was scheduled to be performed in phase IV of this program but has been discontinued due to a lack of funding.

References

1. Saxer, A. P. and Felici, H. M., “Numerical Analysis of 3-D Unsteady Hot Streak Migration and Shock Interaction in a Turbine Stage,” ASME Paper 94-GT-76, International Gas Turbine and Aeroengine Congress and Exposition, The Hague, Netherlands, June 1994.
2. Dorney, D. J., Davis, R. L. and Edwards, D. E., “Unsteady Analysis of Hot Streak Migration in a Turbine Stage,” *Journal of Propulsion and Power*, Vol. 8, No. 2, March-April 1992, pp. 520-529.
3. Rai, M. M. and Dring, R. P., “Navier-Stokes Analyses of the Redistribution of Inlet Temperature Distortions in a Turbine,” *Journal of Propulsion and Power*, Vol. 6, May-June 1990.
4. Takahashi, R. and Ni, R. H., “Unsteady Hot Streak Simulation Through 1-1/2 Stage Turbine,” AIAA Paper 91-3382, 1991.
5. Adamczyk, J. J., “Model Equation for Simulating Flows in Multistage Turbomachinery,” ASME paper 85-GT-226, Gas Turbine Conference and Exhibit, Houston, TX, March 18-21, 1985.
6. Davis, R. L., Shang, T., Buteau, J. and Ni, R. H., “Prediction of 3-D Unsteady Flow in Multi-Stage Turbomachinery Using an Implicit Dual Time-Step Approach,” AIAA Paper 96-2565, 1996.
7. Ni, R. H., “A Multiple Grid Scheme for Solving the Euler Equations,” *AIAA Journal,* Vol. 20, No. 11, pp. 1565-1571, 1981.

8. Ni, R. H. and Bogoian, J. C., “Predictions of 3-D Multi-Stage Turbine Flow Fields Usin a Multiple-Grid Euler Solver,” AIAA Paper 89-0203, 1989.
9. Ni, R. H. and Sharma, O. P., “Using a 3-D Euler Flow Simulation to Assess Effects of Periodic Unsteady Flow Through Turbines,” AIAA Paper 90-2357, 1990.
10. Baldwin, B. S. and Lomax, H., “Thin Layer Approximation and Algebraic Model for Separated Turbulent Flows,” AIAA paper 78-257, 16th Aerospace Sciences Meeting, Jan. 16-18, 1978, Huntsville, AL.
11. Giles, M., “Nonreflecting Boundary Conditions for Euler Equation Calculations,” *AIAA Journal*, Vol. 28, No. 12, pp. 2050-2058, 1990.
12. Sondak, D. L., Dorney, D. J. and Davis, R. L., “Modeling Turbomachinery Unsteadiness with Lumped Deterministic Stresses,” AIAA Paper 96-2570, 32nd Joint Propulsion Conference, Lake Buena Vista, FL, July 1996.

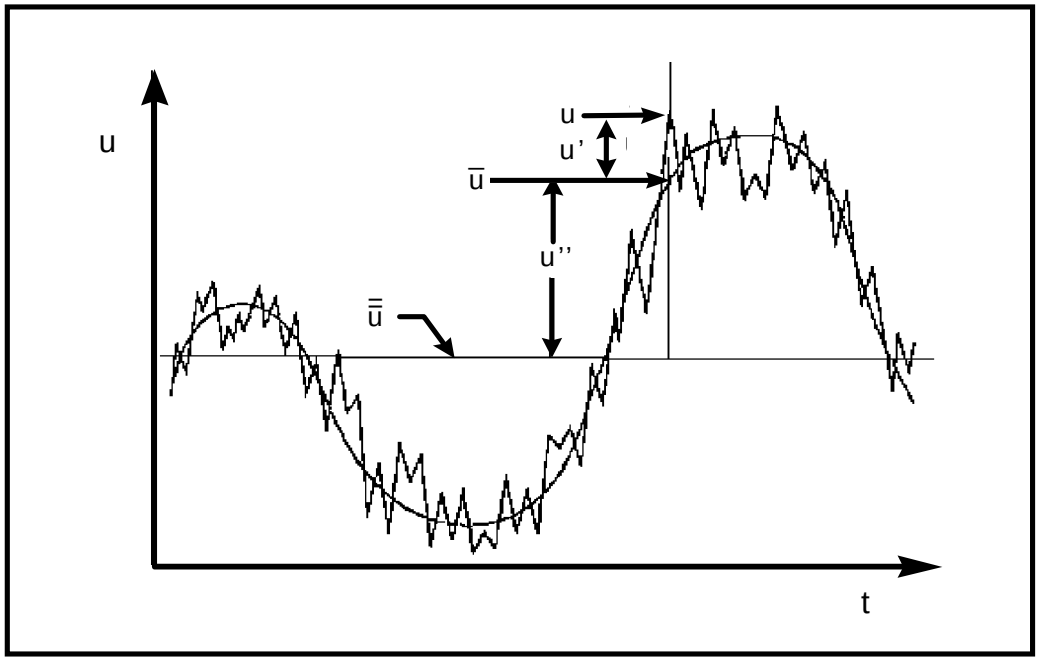

Figure1. Unsteady velocity decomposition.

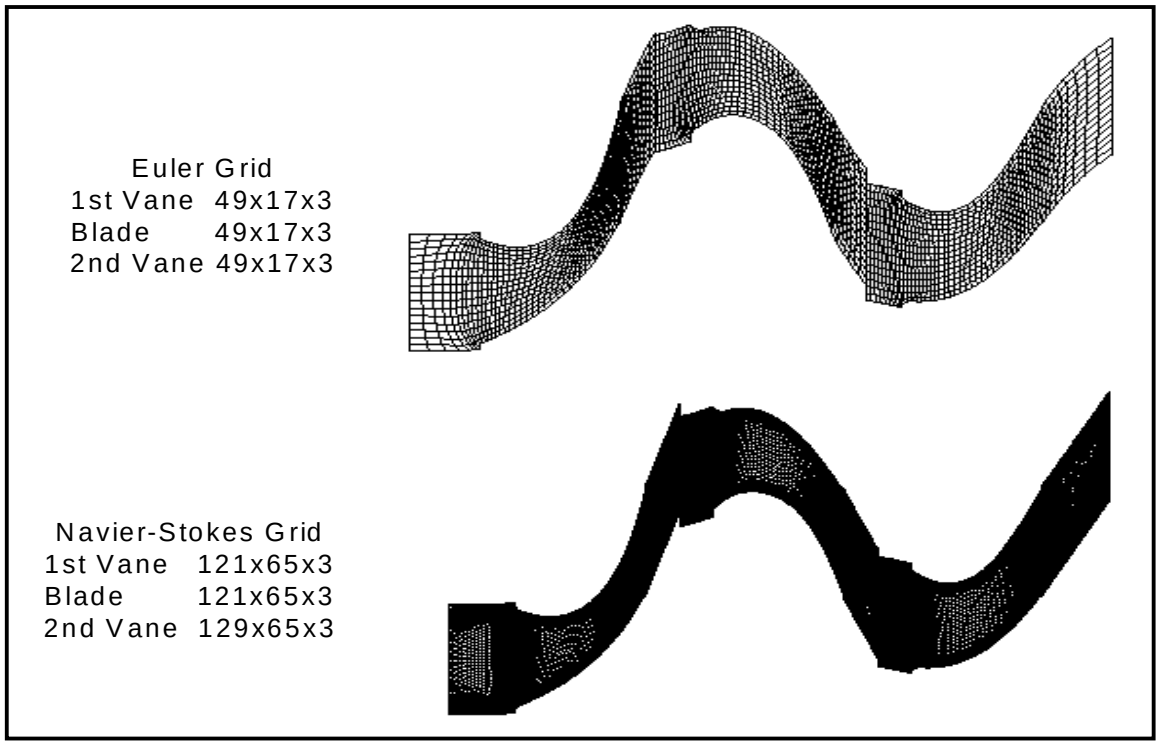

Figure 2. Two dimensional inviscid and viscous grid distributions for a 1 ½ stage turbine.

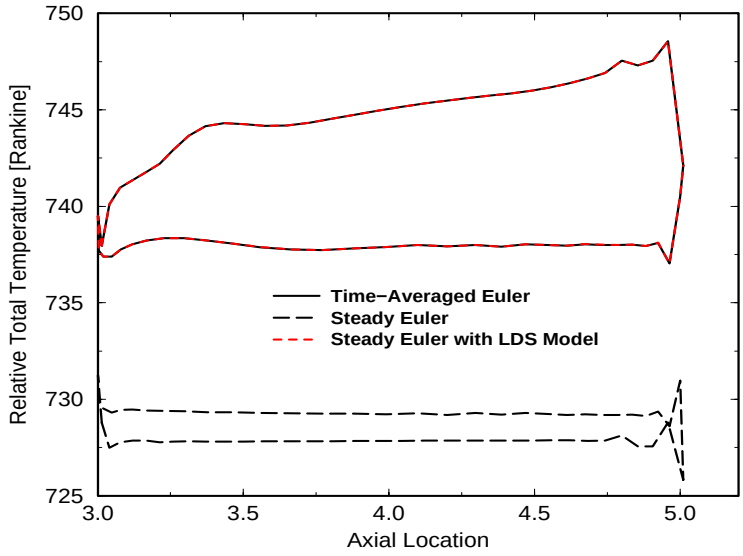

Figure 3. Two-dimensional LDS terms applied to inviscid steady simulation exactly reproduce the time-averaged relative total temperature distribution on the blade surface.

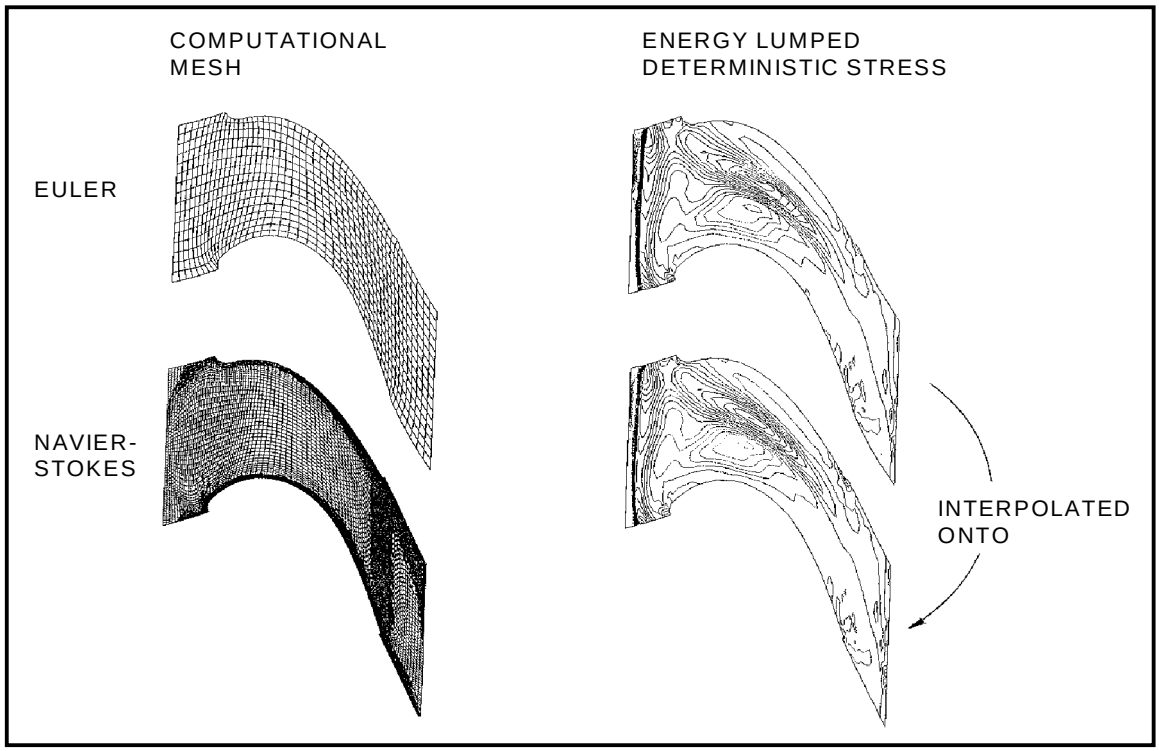

Figure 4. Two-dimensional inviscid LDS field (energy field shown) are interpolated from the inviscid to viscous mesh.

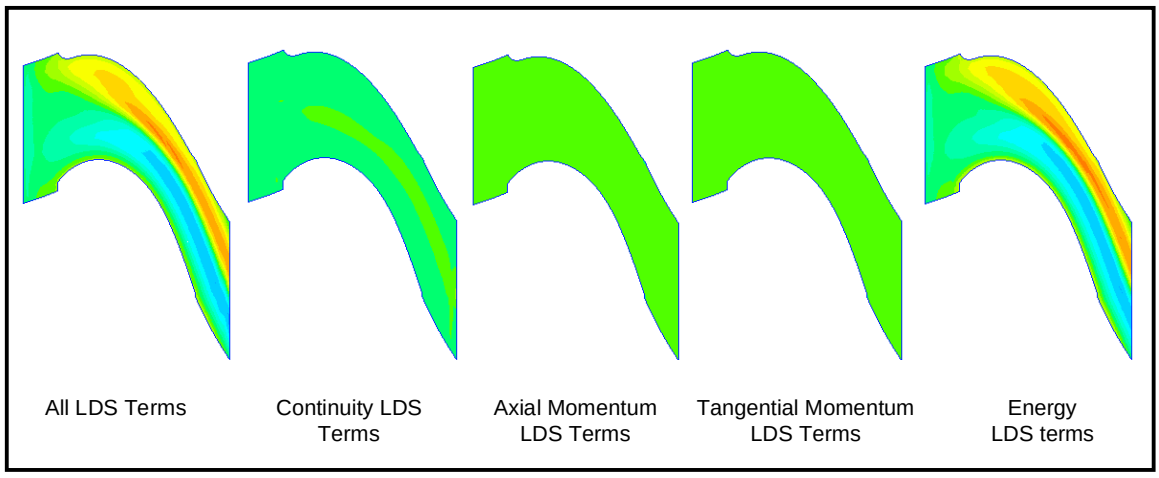

Figure 5. The hot streak migration and segregation are dominated by the energy LDS terms.

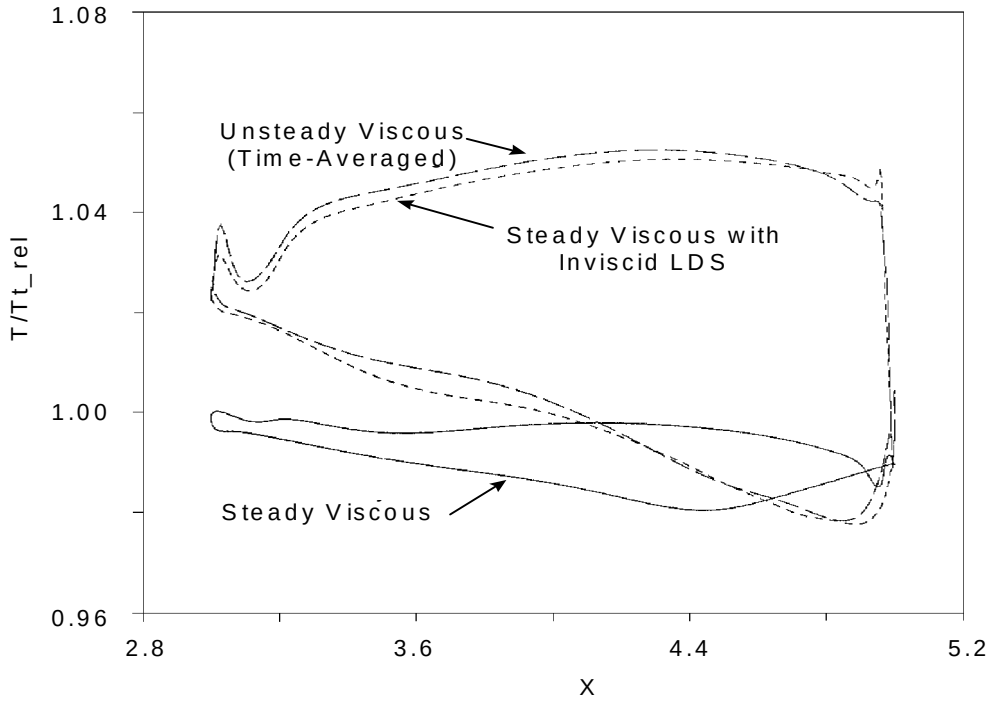

Figure 6. Inviscid LDS field applied to steady two-dimensional viscous simulation reproduces the time-averaged relative total temperature distribution on the rotor blade.

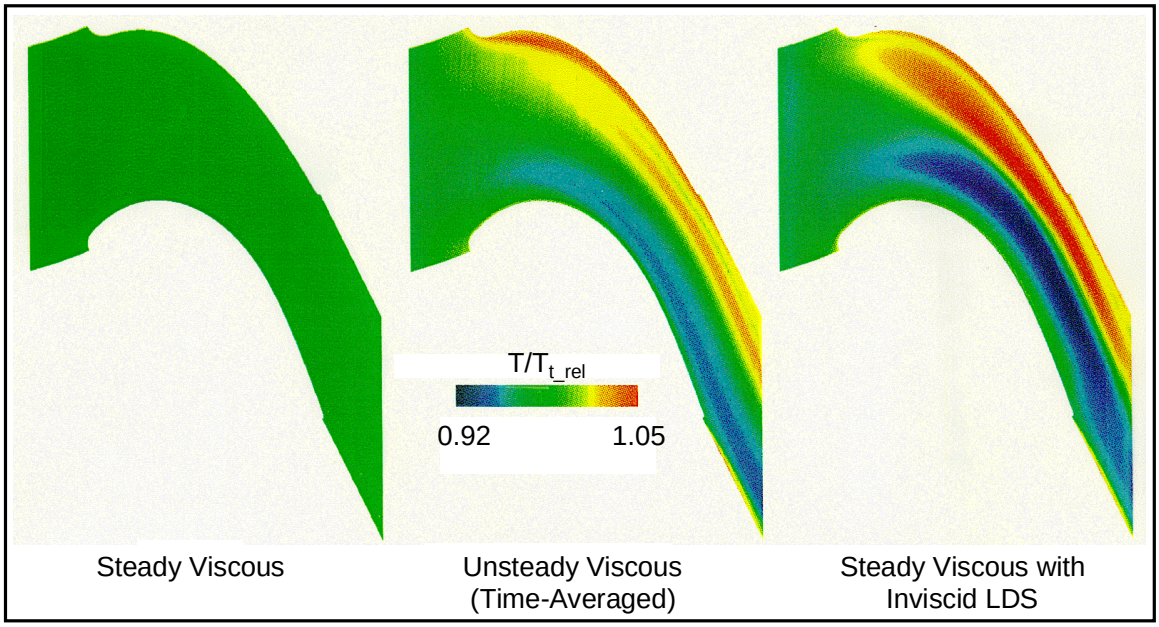

Figure 7. Inviscid LDS terms applied to a steady two-dimensional viscous simulation reproduce the time-averaged segregation of the relative total temperature in the rotor blade.

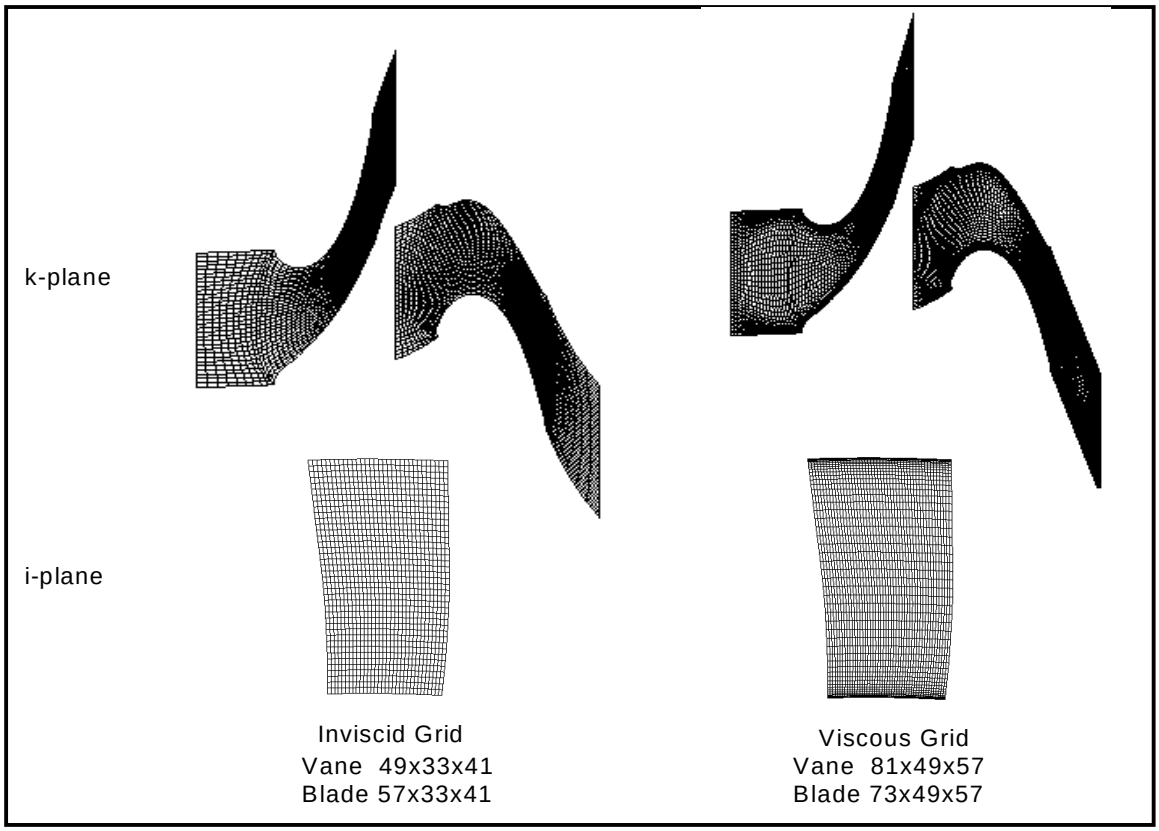

Figure 8. Inviscid and viscous grid distributions for three-dimensional application.

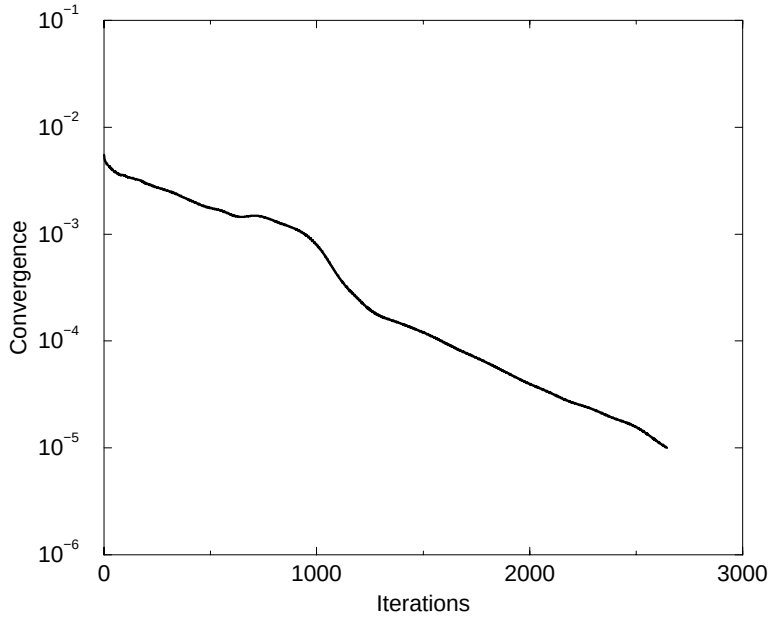

Figure 9. The convergence history for steady inviscid solution with inviscid LDS model indicates that the addition of the LDS source terms does not cause instabilities in the solution.

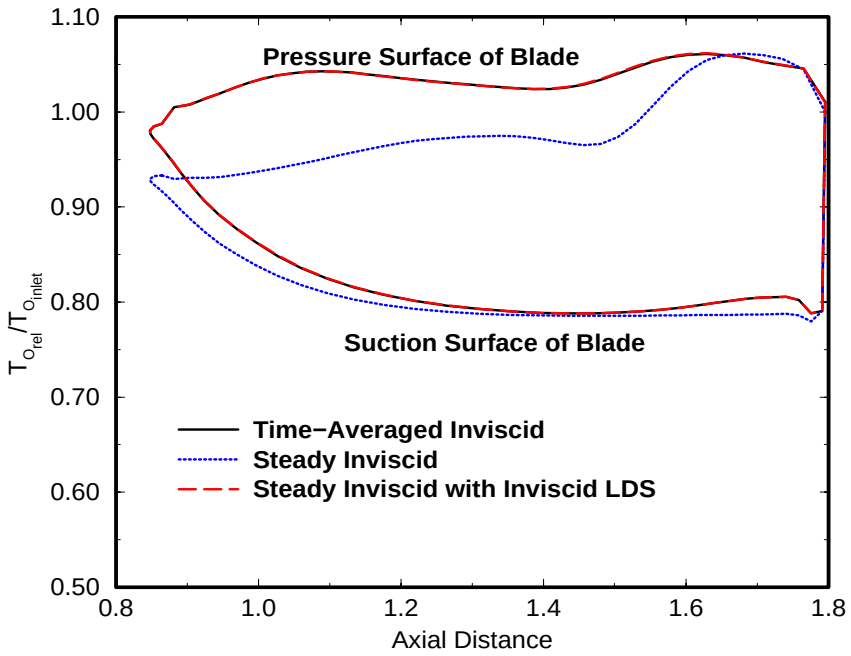

10a.) 20% span

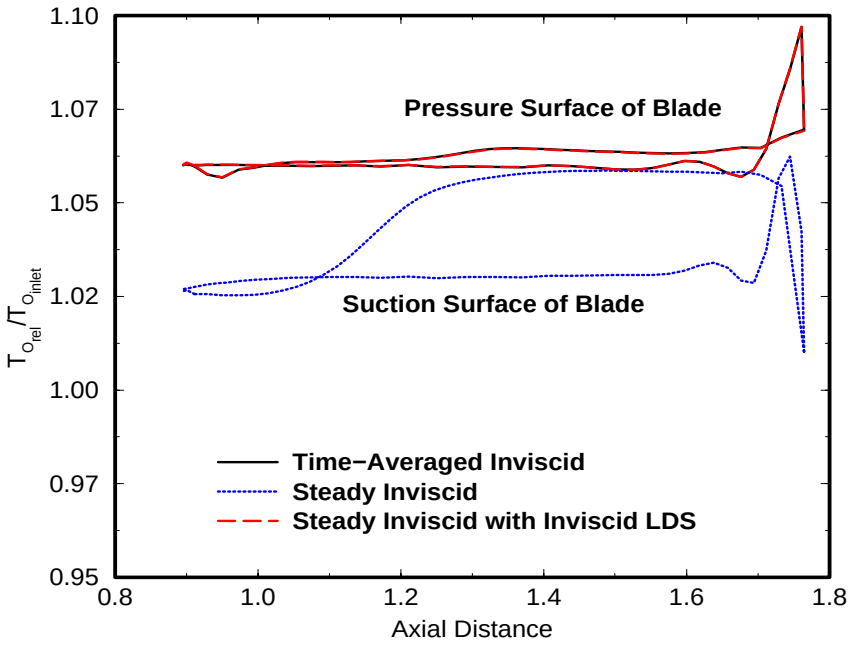

10b.) 50% span

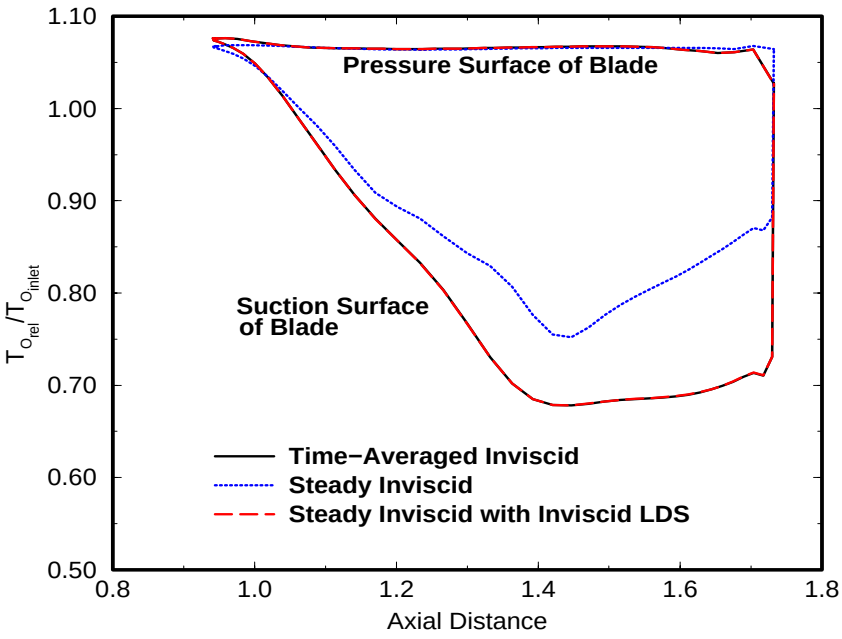

10c.) 80% span

Figure 10. Three-dimensional inviscid LDS model applied to an inviscid steady simulation EXACTLY reproduces the time-averaged relative total temperature distribution on the rotor blade.

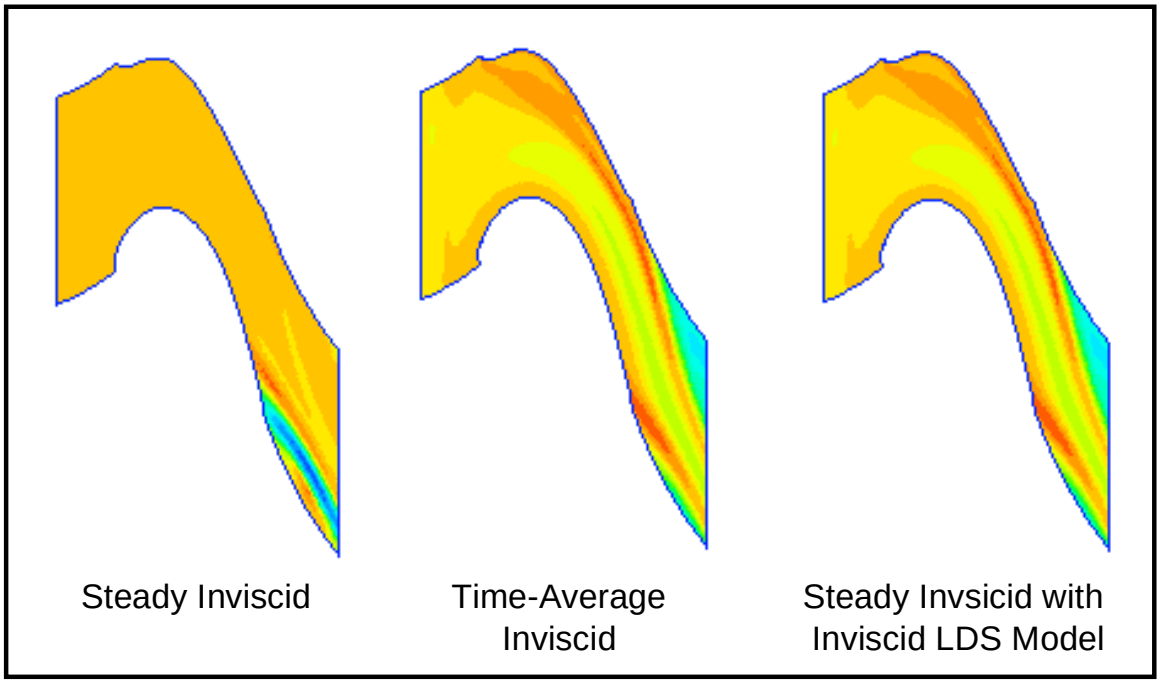

Figure 11. Three-dimensional inviscid LDS field applied to an inviscid steady simulation EXACTLY reproduces the time-averaged relative total temperature segregation in the passage at midspan.

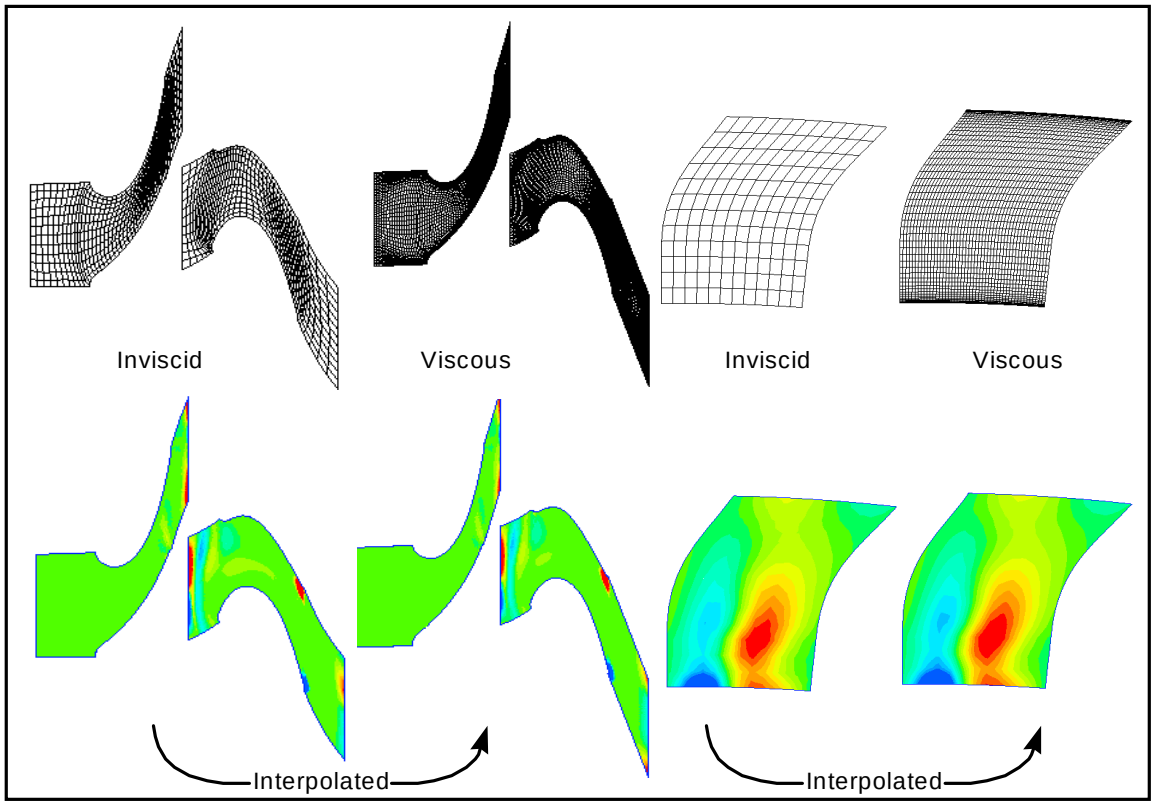

Figure 12. Three-dimensional energy deterministic stress field from inviscid grid interpolated onto viscous grid.

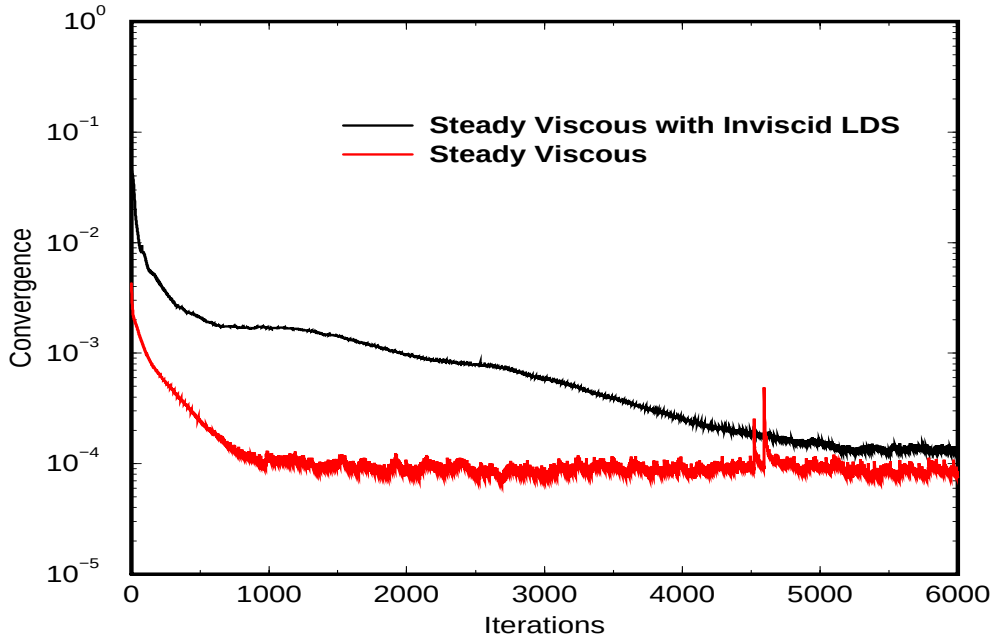

Figure 13. The convergence history for the steady three-dimensional viscous solution with inviscid LDS model shows that the additional source term does not cause instabilities in the solution.

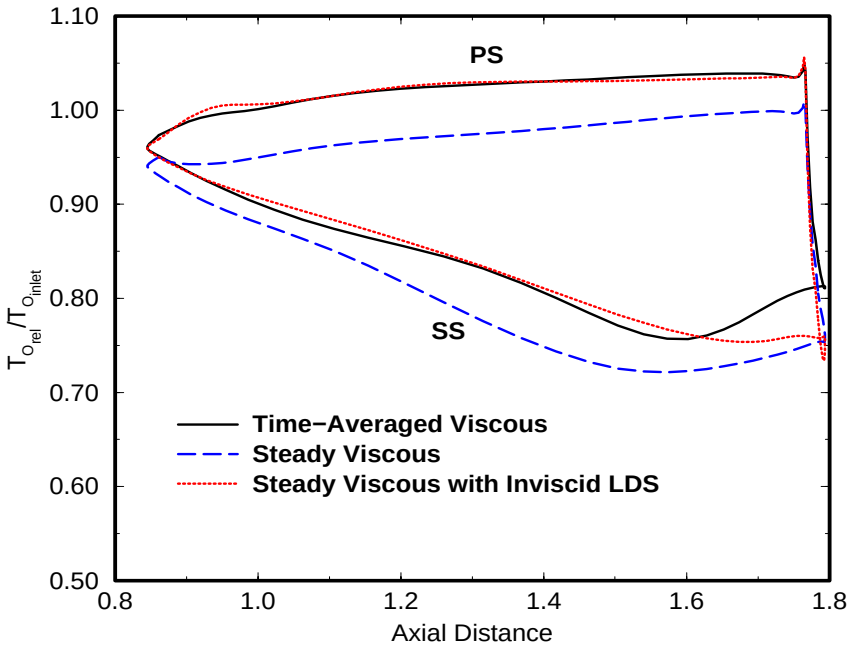

14a.) 20% span

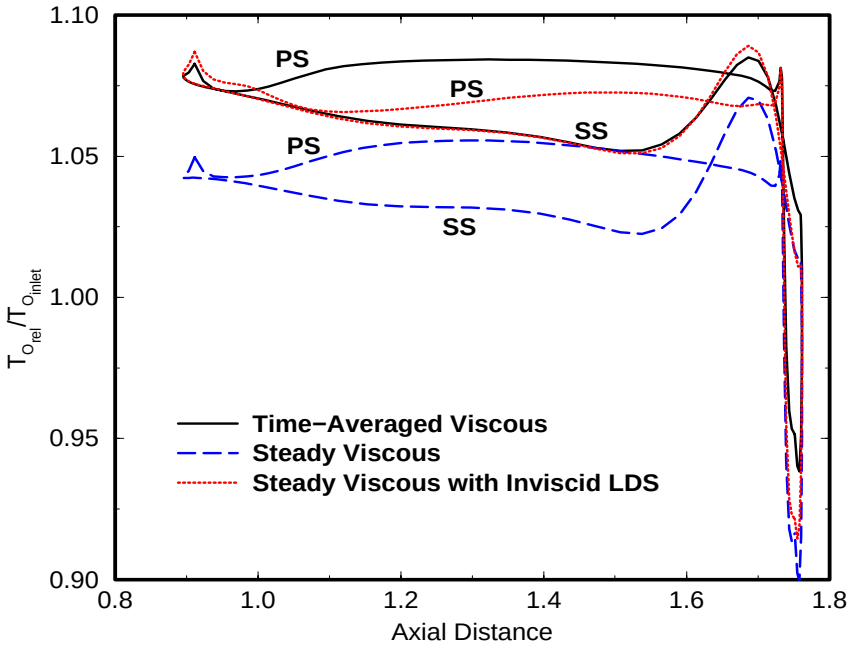

14b.) 50% span

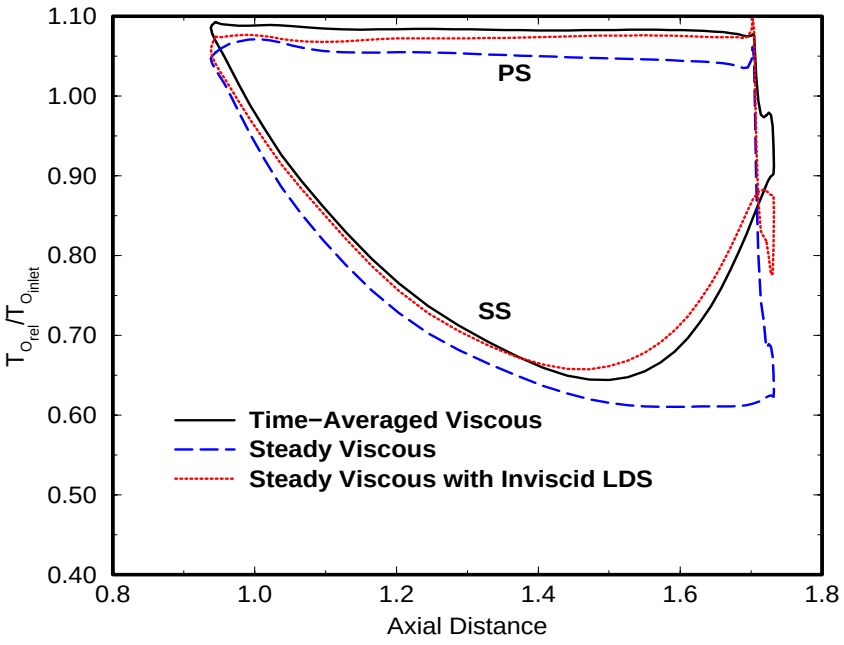

14c.) 80% span

Figure 14. Three-dimensional steady viscous solution with inviscid LDS model does a good job of reproducing the time-averaged relative total temperature distribution on the blade.

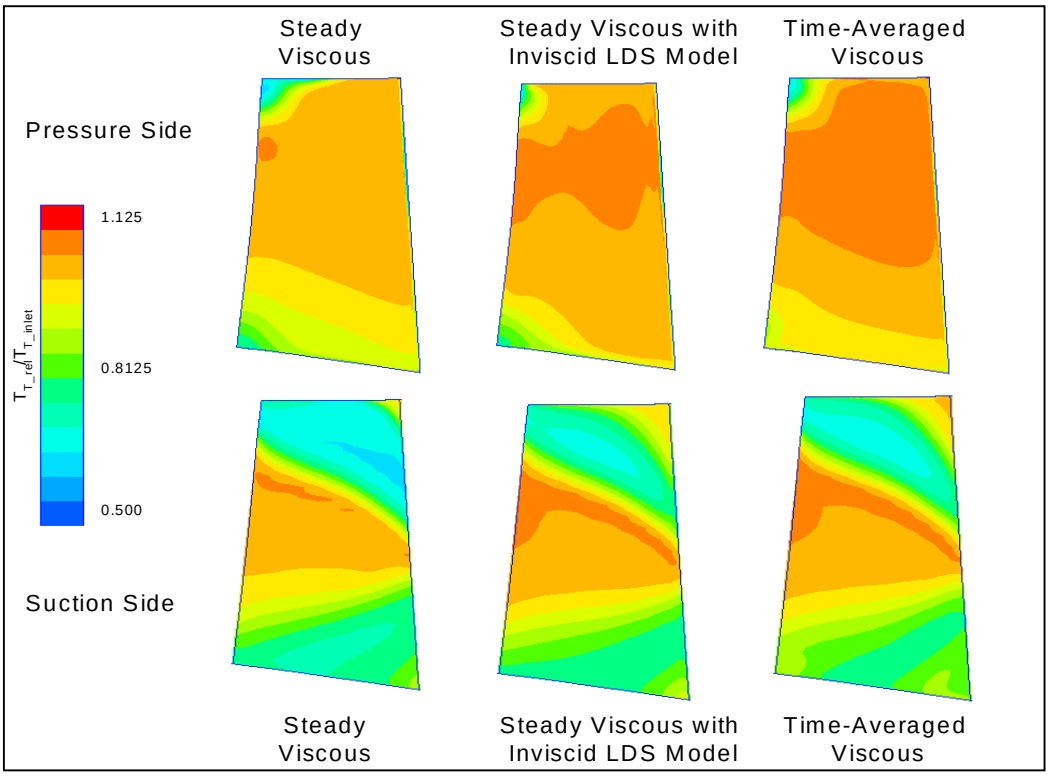

Figure 15. The relative total temperature contours on the rotor surface indicate that the inviscid LDS model predicts the time-averaged accumulation of the hot streak on the pressure side, but under-predicts the spreading of the hot streak.

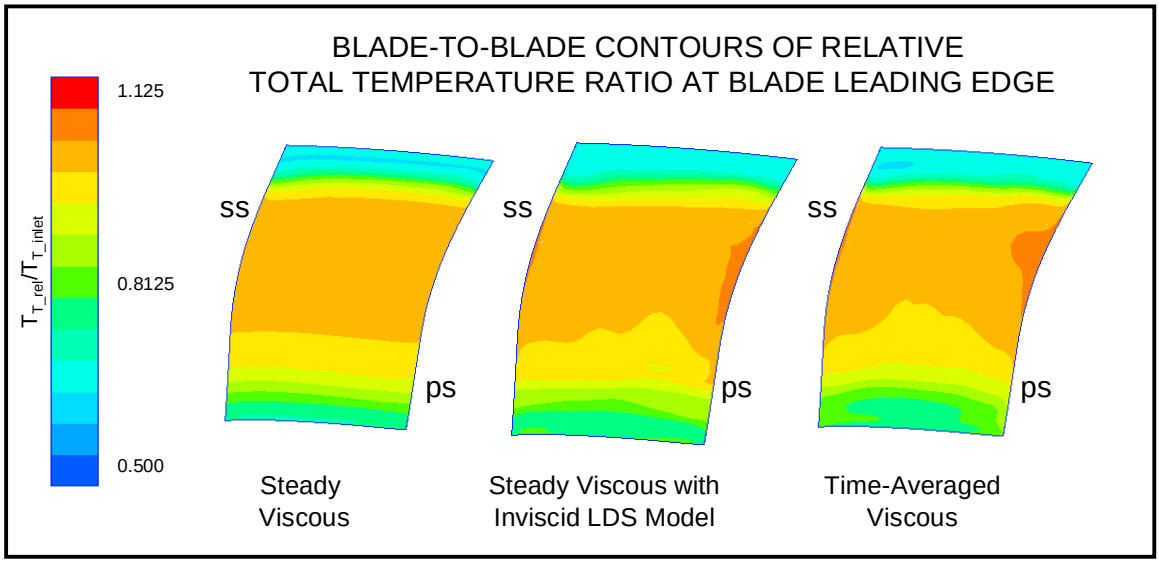

Figure 16. The inviscid LDS model reproduces the time-averaged viscous relative total temperature segregation at the leading edge that is not produced by the steady viscous solution.

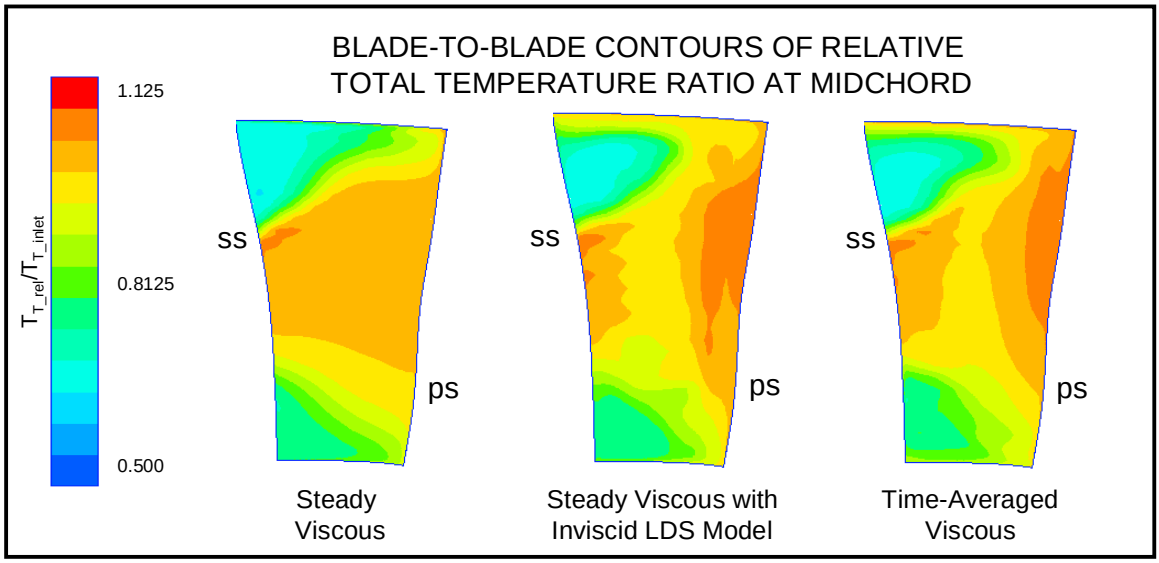

Figure 17. The LDS model reproduces the time-averaged viscous relative total temperature segregation, but the core of the hot streak predicted with the LDS model is less concentrated than that of the time-averaged hot streak core.

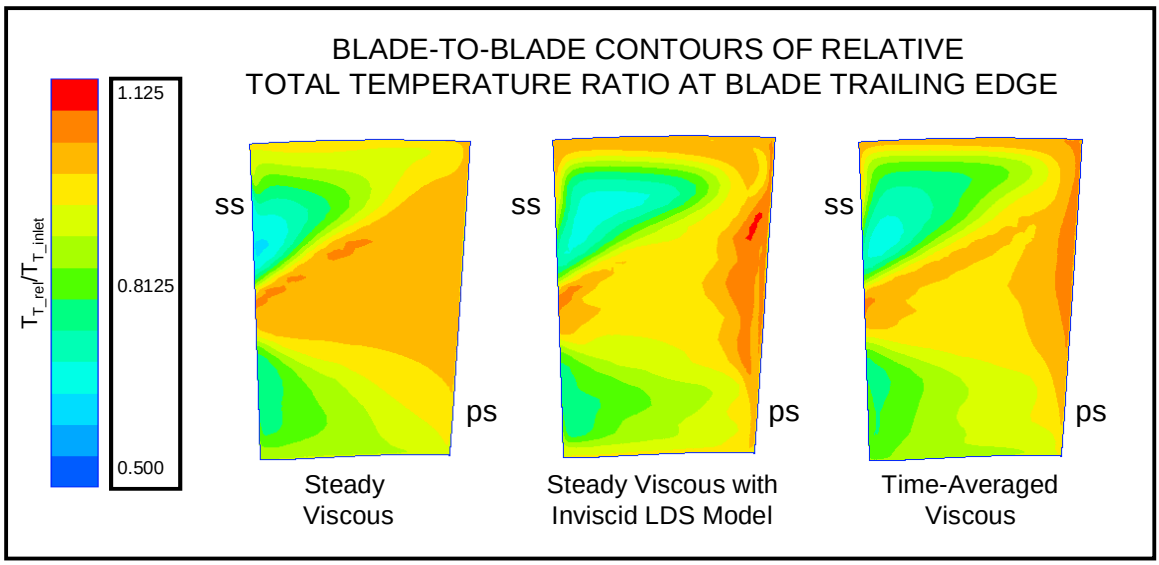

Figure 18. The inviscid LDS model indicates that that the hot streak completely segregates by the time it reaches the trailing edge, while the time-averaged viscous flow shows some hot flow in the core region.

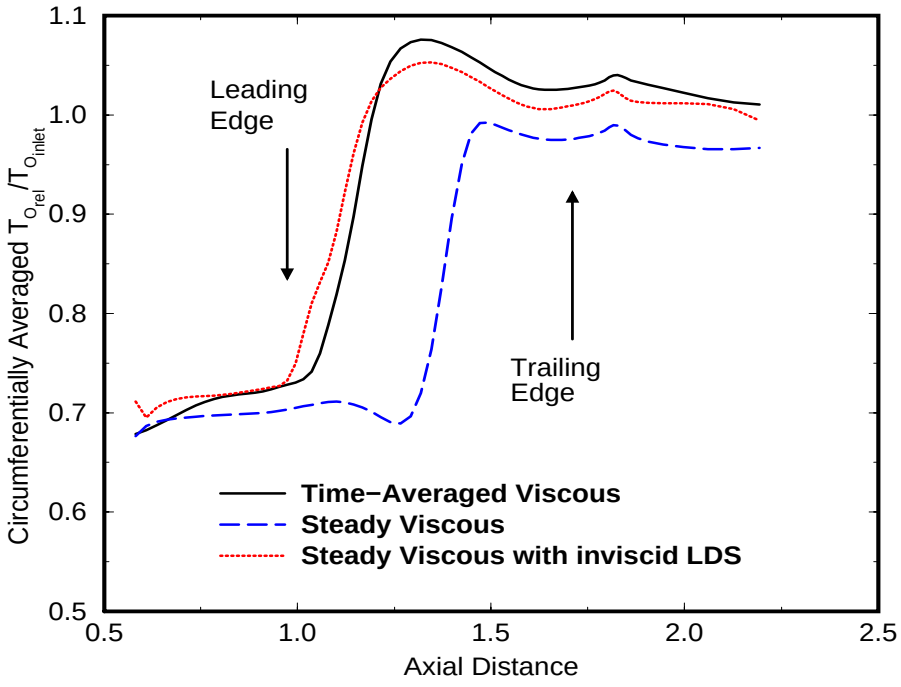

Figure 19. The inviscid LDS model shows the same relative total temperature levels and location of increased heating on the outer air seal as the time-averaged viscous relative total temperature distribution, while the steady viscous solution under-predicts the temperature at all axial locations and delays the heat buildup until almost mid-chord.

REPORT DOCUMENTATION PAGE

Form Approved
OMB No. 0704-0188

1. AGENCY USE ONLY (*Leave blank*)	2. REPORT DATE	3. REPORT TYPE AND DATES COVERED
	October 1998	Final Contractor Report

4. TITLE AND SUBTITLE

Deterministic Stress Modeling of Hot Gas Segregation in a Turbine

5. FUNDING NUMBERS

WU–509–10–11–00
NAS3–26618 Task Order 28

6. AUTHOR(S)

Judy Busby, Doug Sondak, Brent Staubach, and Roger Davis

7. PERFORMING ORGANIZATION NAME(S) AND ADDRESS(ES)

United Technologies Research Center, Pratt & Whitney
411 Silver Lane
East Hartford, Connecticut 06108

8. PERFORMING ORGANIZATION REPORT NUMBER

E–11377

9. SPONSORING/MONITORING AGENCY NAME(S) AND ADDRESS(ES)

National Aeronautics and Space Administration
Lewis Research Center
Cleveland, Ohio 44135–3191

10. SPONSORING/MONITORING AGENCY REPORT NUMBER

NASA CR—1998-208666
UTRC Report 98–07

11. SUPPLEMENTARY NOTES

Project Manager, Joseph P. Veres, Computing and Interdisciplinary Systems Office, NASA Lewis Research Center, organization code 2900, (216) 433–2436.

12a. DISTRIBUTION/AVAILABILITY STATEMENT

Unclassified - Unlimited
Subject Categories: 77 and 66 Distribution: Nonstandard

This publication is available from the NASA Center for AeroSpace Information, (301) 621–0390.

12b. DISTRIBUTION CODE

13. ABSTRACT ***(Maximum 200 words)***

Simulation of unsteady viscous turbomachinery flowfields is presently impractical as a design tool due to the long run times required. Designers rely predominantly on steady-state simulations, but these simulations do not account for some of the important unsteady flow physics. Unsteady flow effects can be modeled as source terms in the steady flow equations. These source terms, referred to as Lumped Deterministic Stresses (LDS), can be used to drive steady flow solution procedures to reproduce the time-average of an unsteady flow solution. The goal of this work is to investigate the feasibility of using inviscid lumped deterministic stresses to model unsteady combustion hot streak migration effects on the turbine blade tip and outer air seal heat loads using a steady computational approach. The LDS model is obtained from an unsteady inviscid calculation. The LDS model is then used with a steady viscous computation to simulate the time-averaged viscous solution. Both two-dimensional and three-dimensional applications are examined. The inviscid LDS model produces good results for the two-dimensional case and requires less than 10% of the CPU time of the unsteady viscous run. For the three-dimensional case, the LDS model does a good job of reproducing the time-averaged viscous temperature migration and separation as well as heat load on the outer air seal at a CPU cost that is 25% of that of an unsteady viscous computation.

14. SUBJECT TERMS	15. NUMBER OF PAGES
Turbine; Computational fluid dynamics; CFD; Simulation	29
	16. PRICE CODE: A03

17. SECURITY CLASSIFICATION OF REPORT	18. SECURITY CLASSIFICATION OF THIS PAGE	19. SECURITY CLASSIFICATION OF ABSTRACT	20. LIMITATION OF ABSTRACT
Unclassified	Unclassified	Unclassified	